CHAPTER 5

RESULTS

Table. II. The powder size-distribution of Tungsten and Copper

Powder Size		% Weight	
microns	BS. Mesh No.	Tungsten	Copper
+106 to -150	+106 to -100	-	0.01
+ 75 to -106	+200 to -106	-	35.95
+ 53 to - 75	+300 to -200	6.04	44.82
+ 45 to - 53	+350 to -300	12.49	9.56
+ 38 to - 45	+400 to -350	25.29	6.85
- 38	-400	56.17	2.67

The selected size of Tungsten powder is -38 microns

The selected size of Copper powder is +53 to -75 microns

Table. III. The average density of the green pellets for each method of determination (Weight to Volume method and gamma transmission method)

W:Cu	Pressure Tons/cm^2	Density (g/cc) (Wt. to Vol.)	Density (g/cc) (gamma)	gamma Dens. to theo.Den. (%)
60:40	8	11.93 ± 0.06	13.98 ± 0.08	92.19
60:40	12	12.28 ± 0.17	15.50 ± 0.06	94.98
80:20	8	13.26 ± 0.03	15.52 ± 0.41	90.06
80:20	12	14.09 ± 0.44	16.11 ± 0.46	93.50

NB. The theoritical density of 60:40 and 80:20 (W:Cu) are 15.16 and 17.23 g/cc, respectively.

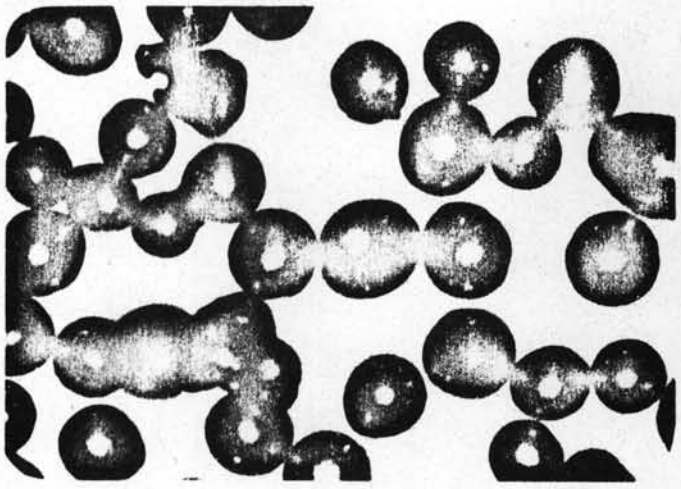

9.a

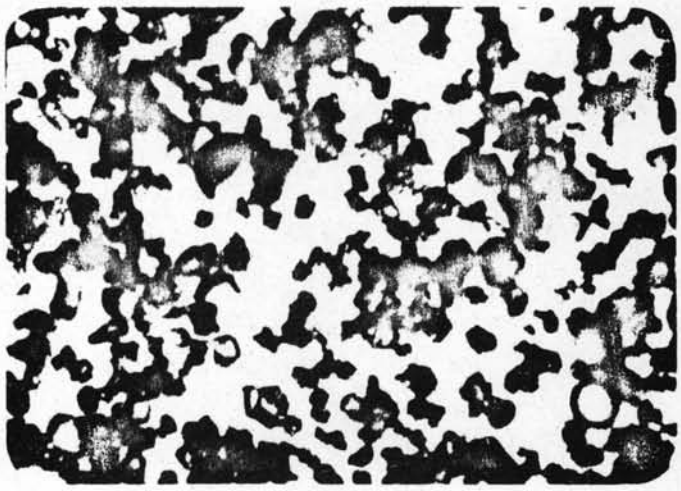

9.b

Fig. 9. Shape of Tungsten and Copper powder before sintering

a. Copper powder X 400

b. Tungsten powder X 400

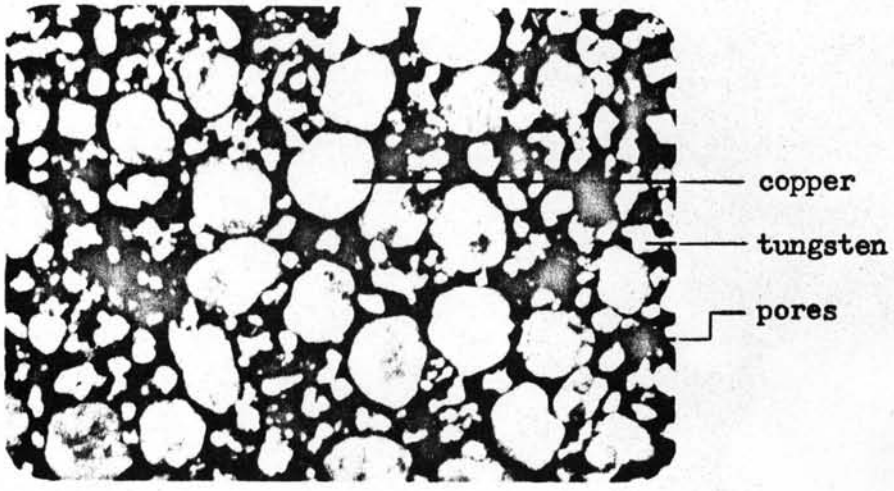

9.c

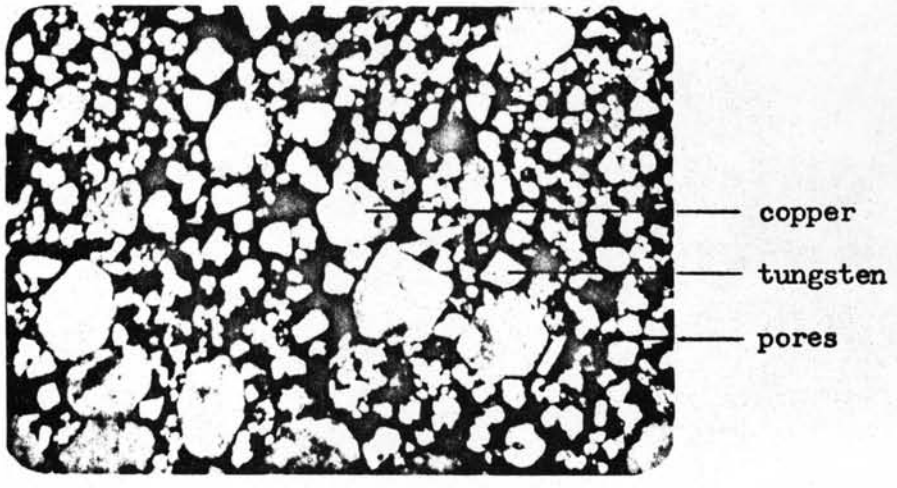

9.d

Fig. 9. Shape of Tungsten and Copper powder before sintering (continued)

c. powder mixture (W:Cu = 60:40) after pressing
X 400

d. powder mixture (W:Cu = 80:20) after pressing
X 400

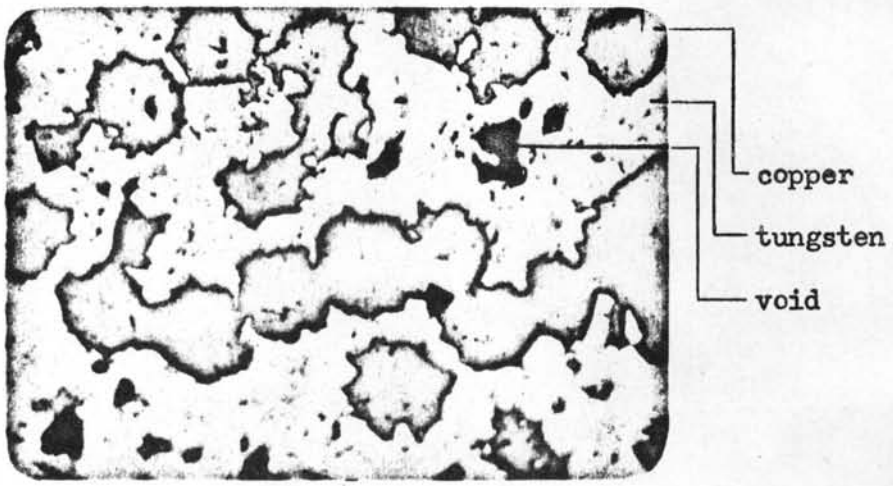

10.a

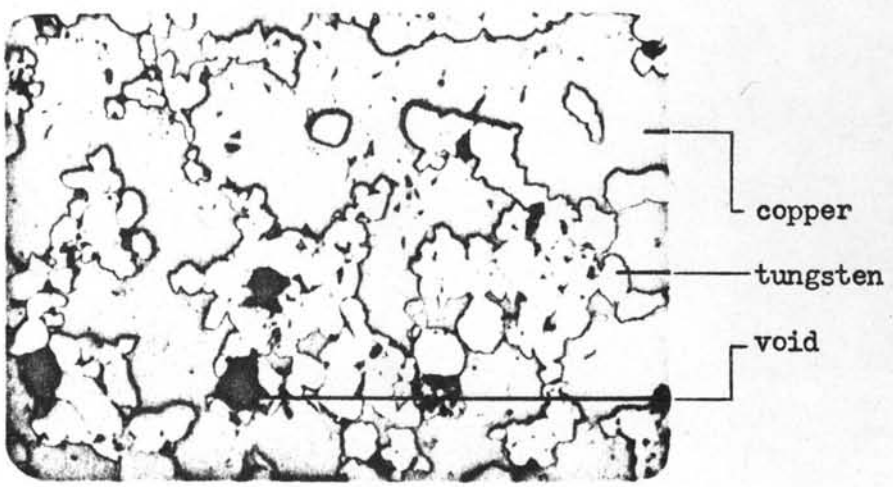

10.b

Fig. 10. The microstructure of the sintered pellets.

a. Solid phase sintering 1000 °C ½ h unetched X 400
(W:Cu = 60:40)

b. Solid phase sintering 1000 °C 2 h unetched X 400
(W:Cu = 60:40)

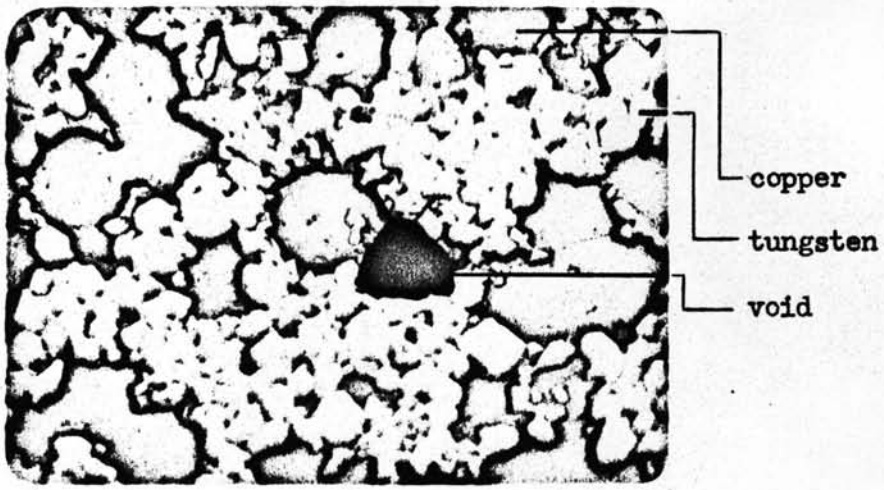

10.c

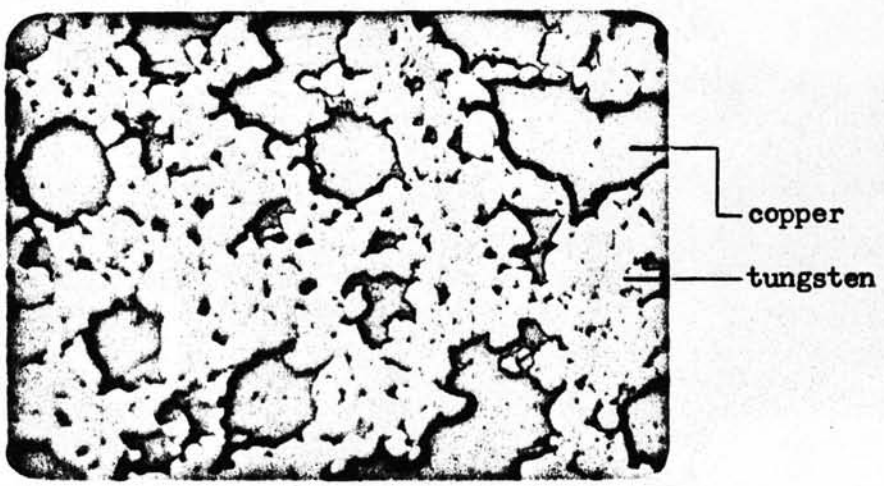

10.d

Fig. 10. The microstructure of the sintered pellets. (continued)

c. Liquid phase sintering 1200 C ½ h unetched X 400
(W:Cu = 80:20)

d. Liquid phase sintering 1200 C 2 h unetched X 400
(W:Cu = 80:20)

Table IV

Relation between Tungsten-Copper content and the photopeak area of each element using the Detection System I.

W : Cu	W counts	Cu counts
0 : 100	-	36670
10 : 90	4417	33335
20 : 80	7749	26942
30 : 70	12005	24042
40 : 60	16113	19291
50 : 50	20449	18495
60 : 40	25576	14731
70 : 30	30548	11630
80 : 20	34742	8490
90 : 10	38695	5342
100 : 0	41697	2211

for Tungsten: $R^2 = 99.54$

$Y = 449.73X - 967.27$

for Copper: $R^2 = 98.84$

$Y = 335.46X + 1515.95$

Table V

Relation between Tungsten-Copper content and the photopeak area of each element using the Detection System II.

W : Cu	W counts	Cu counts
0 : 100	-	1583432
10 : 90	46785	1274625
20 : 80	87656	1081546
30 : 70	133314	940086
40 : 60	182917	702378
50 : 50	227376	698617
60 : 40	274003	514935
70 : 30	307951	391316
80 : 20	357218	268855
90 : 10	389456	114420
100 : 0	432264	-

for Tungsten: R^2 = 99.84

$Y = 4317.07X + 6455.33$

for Copper: R^2 = 97.58

$Y = 15146.58 - 76041.07$

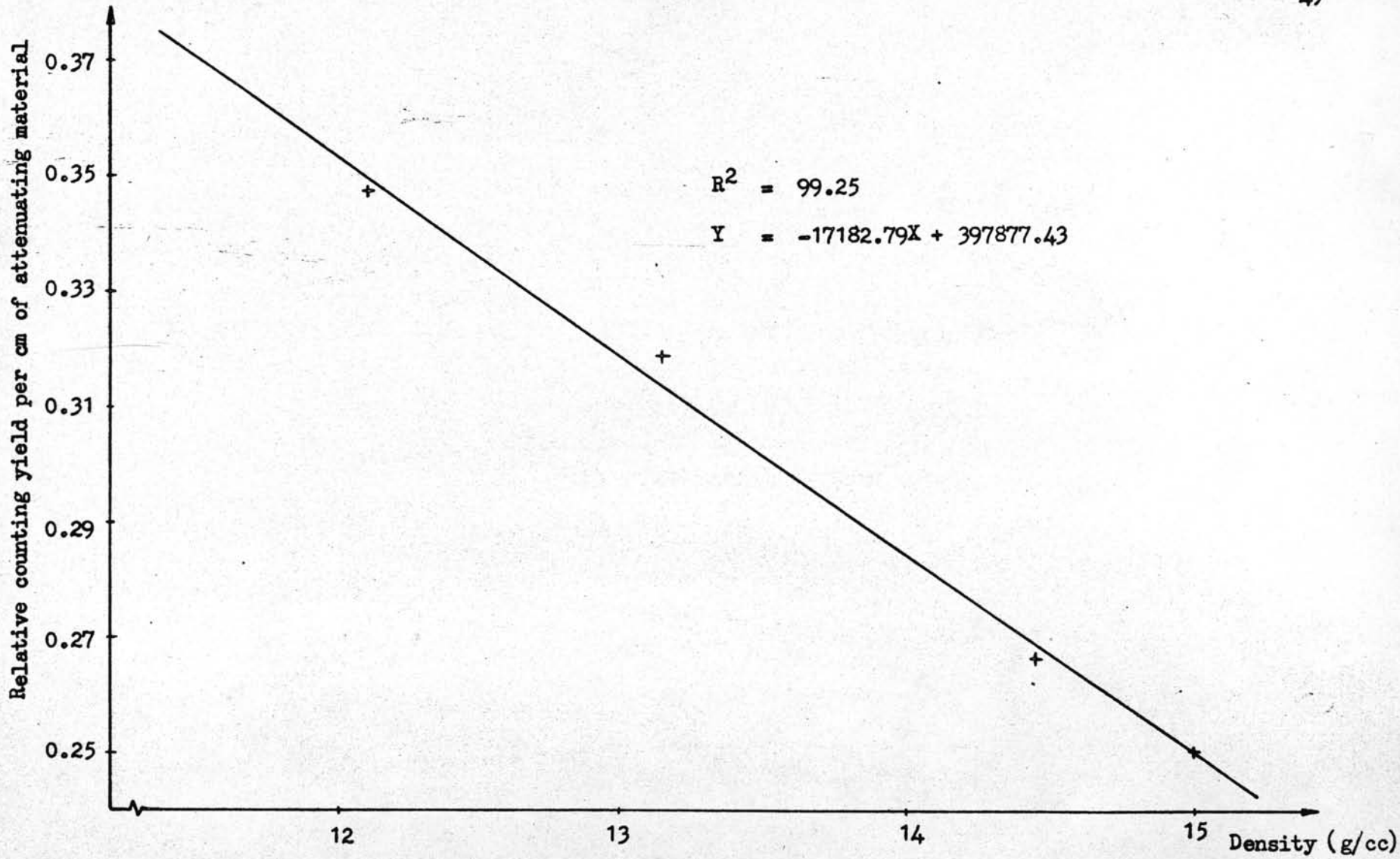

Fig. 11 Calibration curve shows relation between attenuated gamma rays (relative counting yield per cm) and density of attenuating material (g/cc)

Fig. 12 Spectrum of Tungsten-187 and Copper-64 peaks using Ge(Li) detector as stated in System I.

Peak 1, Gamma Energy 0.479 MeV (Tungsten Peak)

Peak 2, Gamma Energy 0.511 MeV (Copper Peak)

Peak 3, Gamma Energy 0.552 MeV (Tungsten Peak)

Peak 4, Gamma Energy 0.618 MeV (Tungsten Peak)

Peak 5, Gamma Energy 0.686 MeV (Tungsten Peak)

Peak 6, Gamma Energy 0.773 MeV (Tungsten Peak)

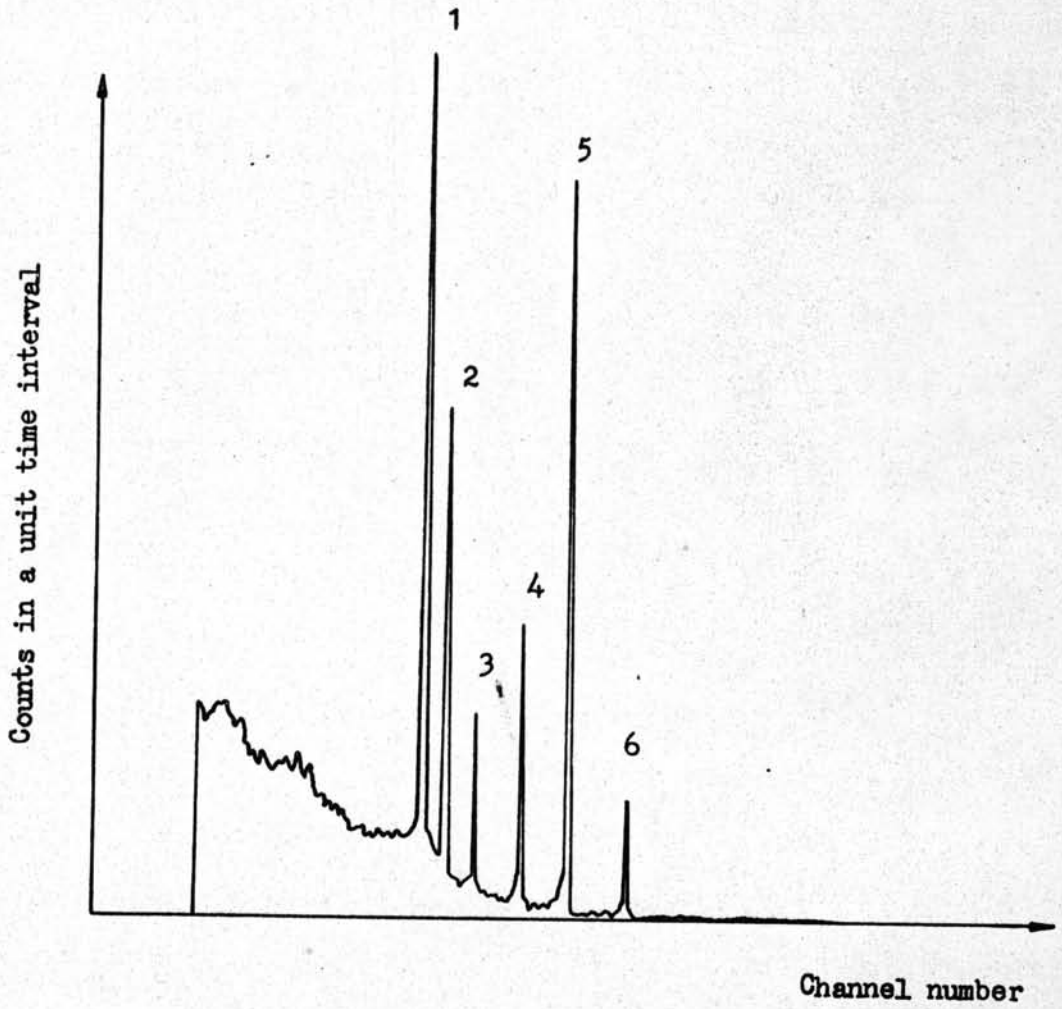

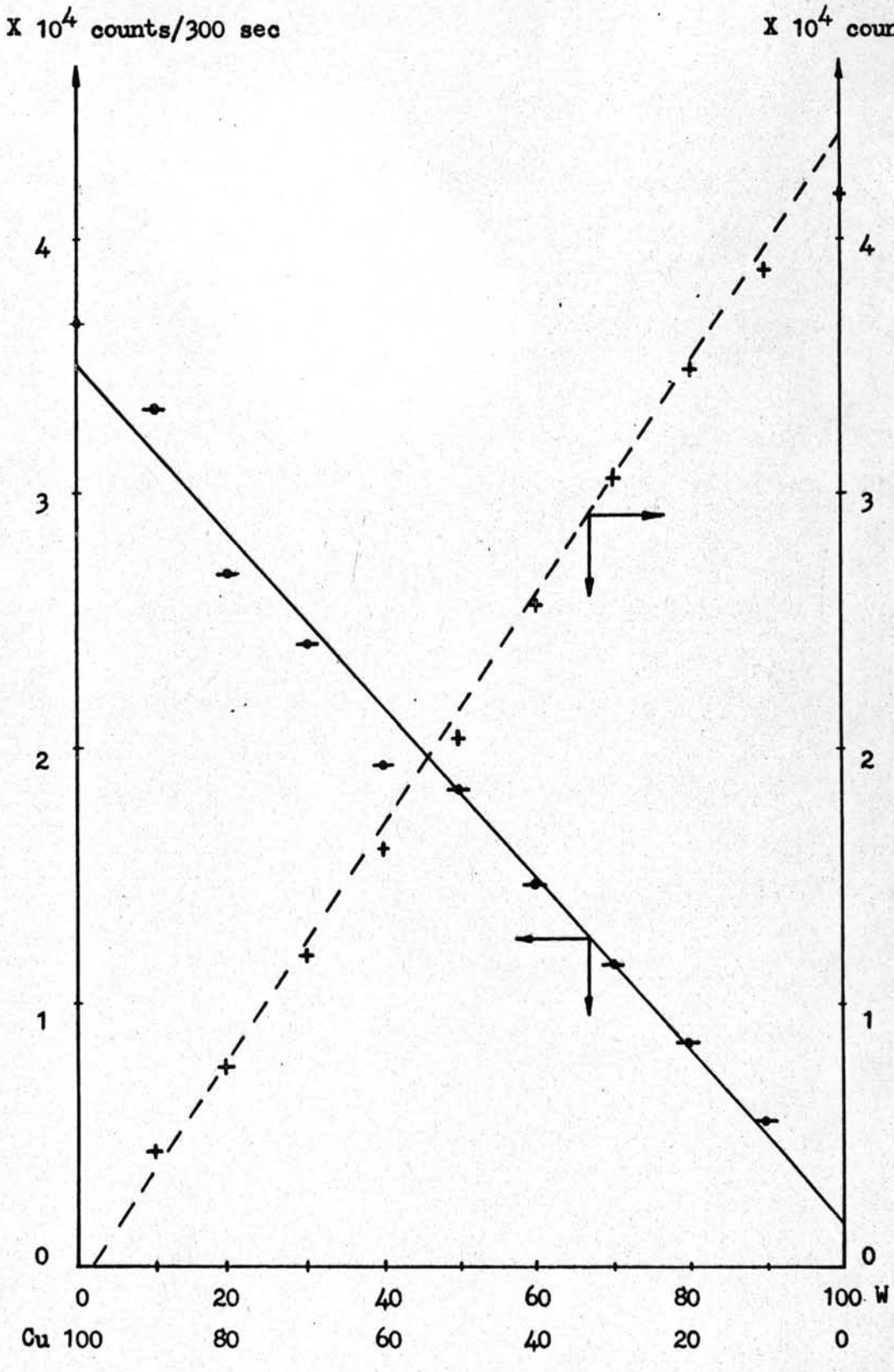

Fig. 13 Graph shows relation between photopeak area and Tungsten-Copper content using Detection System I.

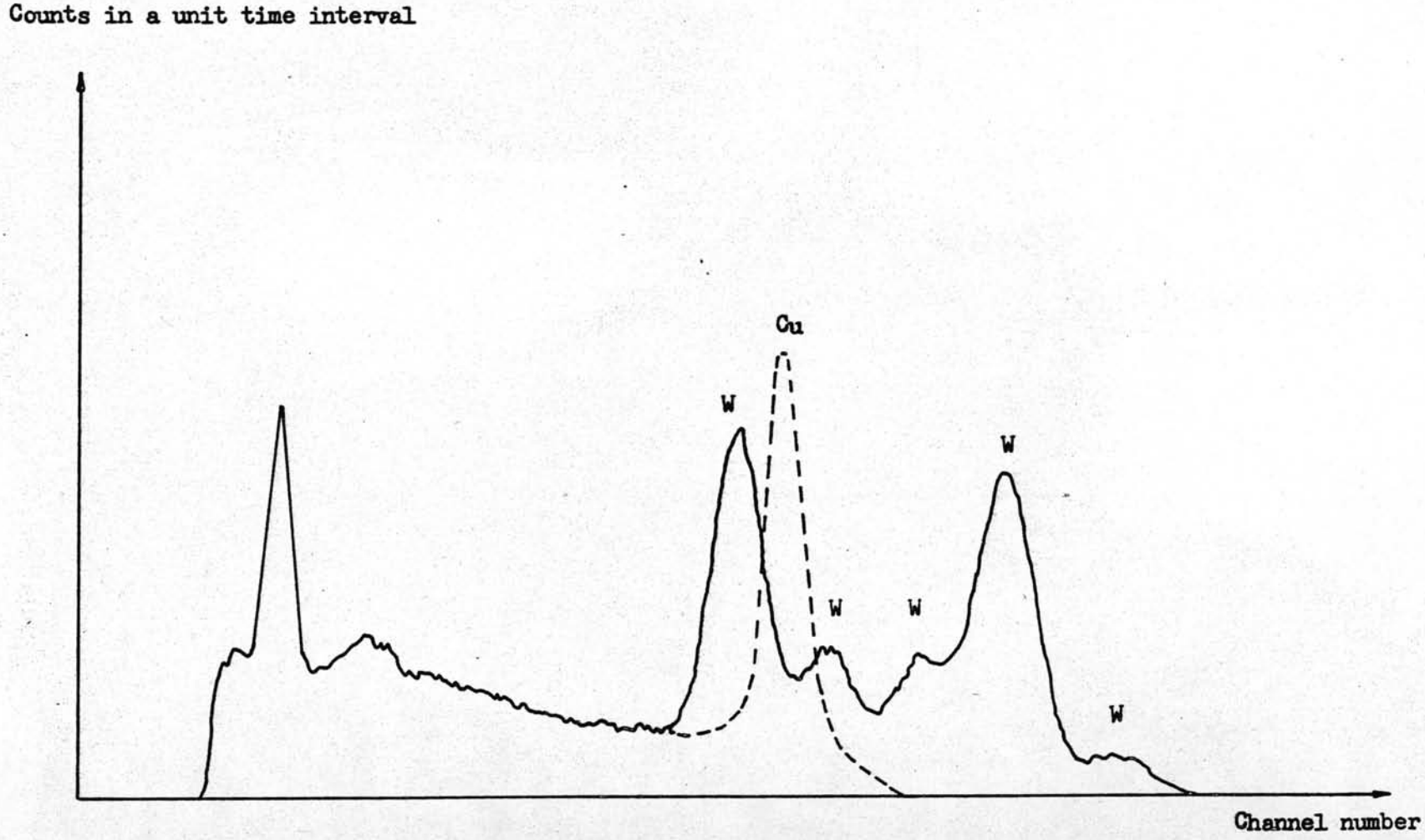

Fig. 14 Spectrum of Tungsten-187 and Copper-64 peaks using NaI(Tl) 3" X 3" Detector as stated in Detection System II.

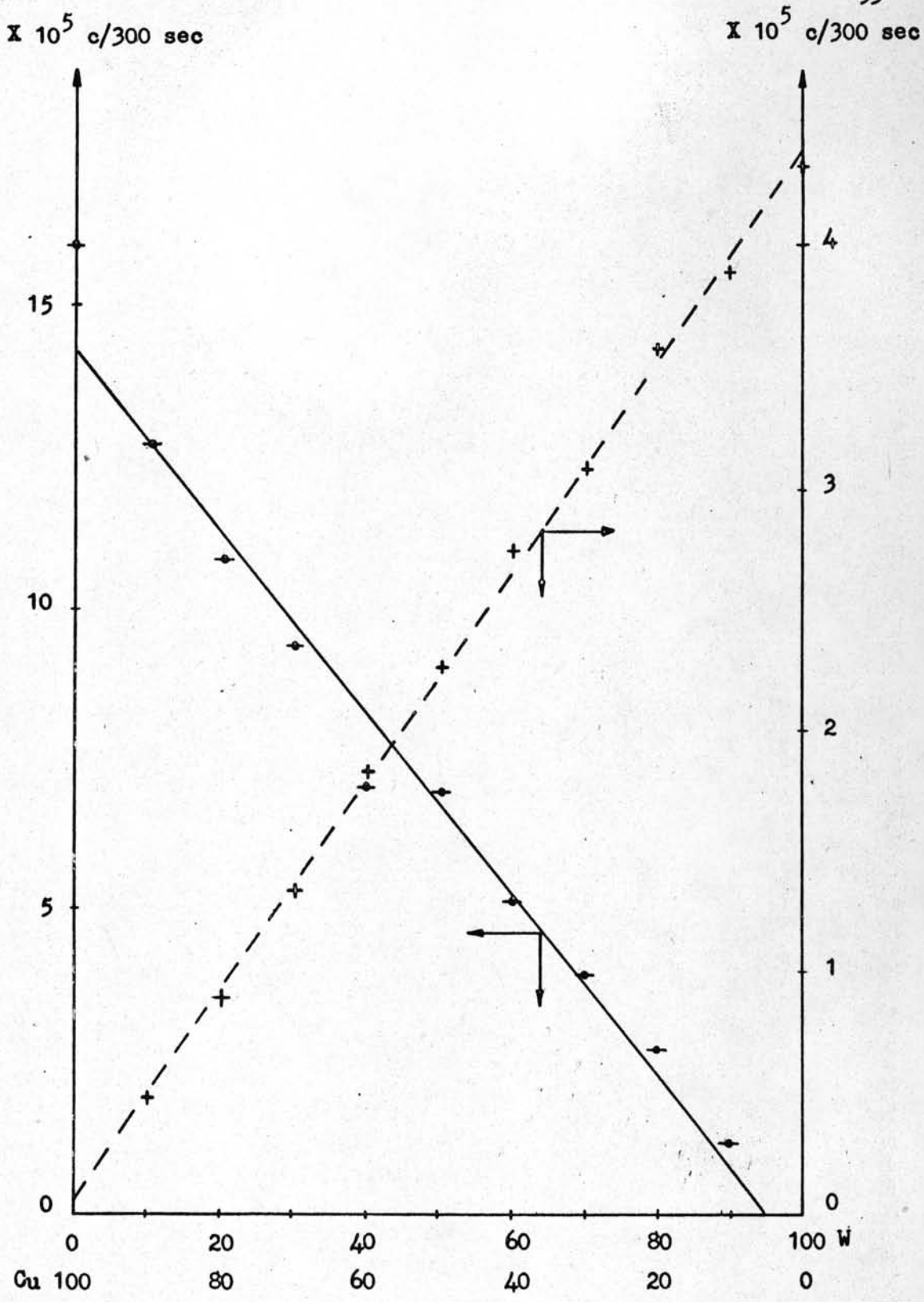

Fig. 15 Graph shows relation between photopeak area and Tungsten-Copper content using Detection System II.

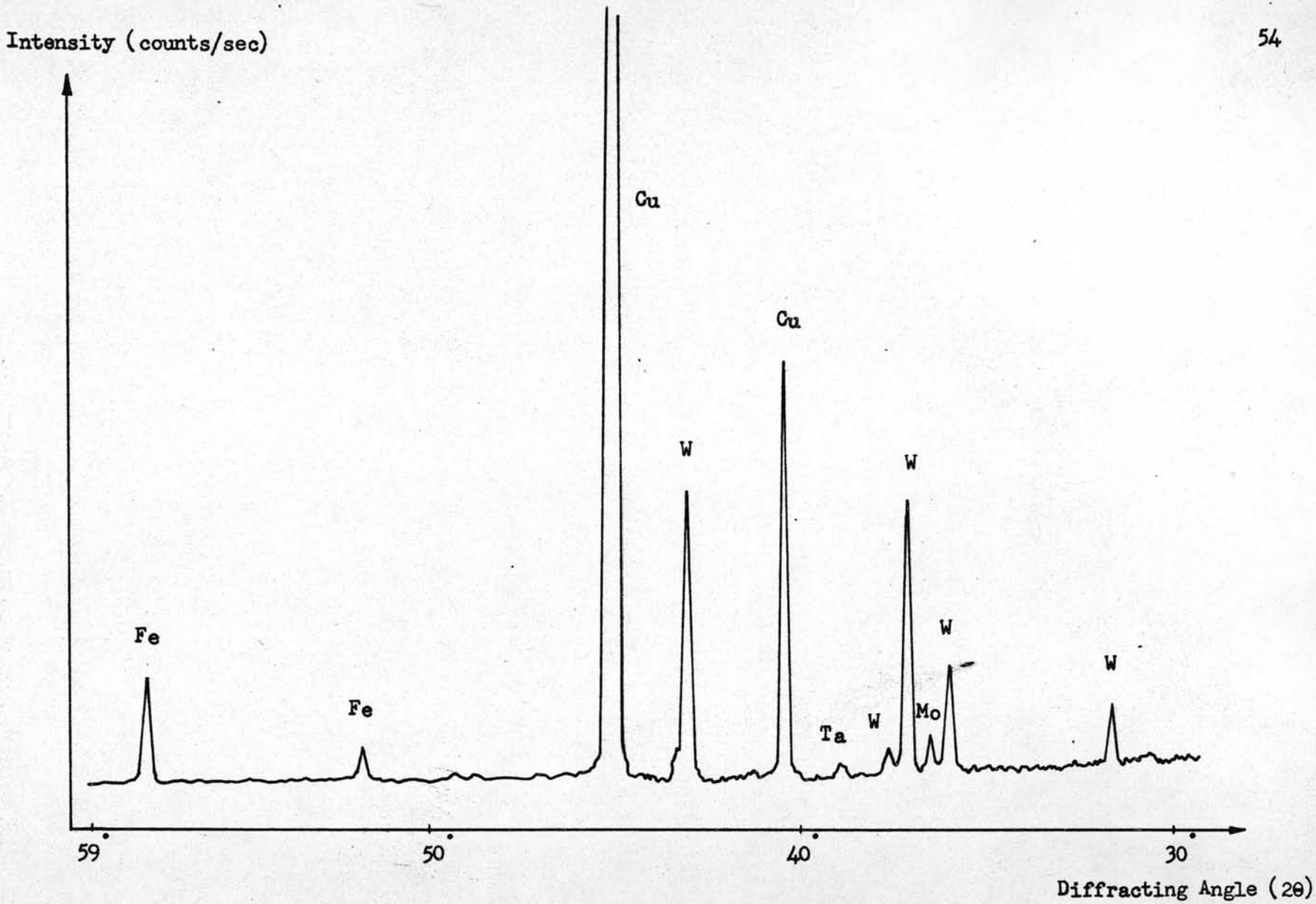

Fig. 16 Spectrum of Tungsten-Copper pellet used in the thesis experiments.

Graph shows relation between X-rays intensities and Diffracting angle (Using System V)

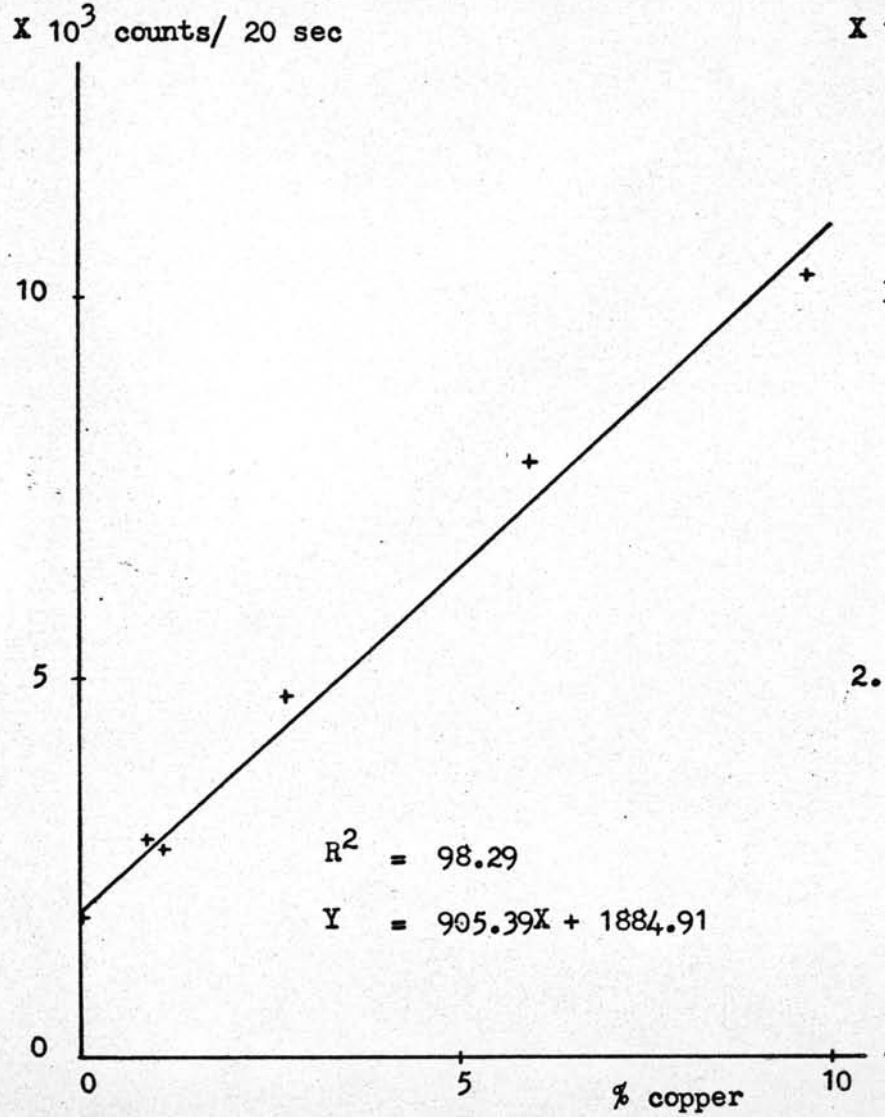

Fig. 17 Calibration curve shows relation between Peak area and % copper in Cast Aluminium Alloys.

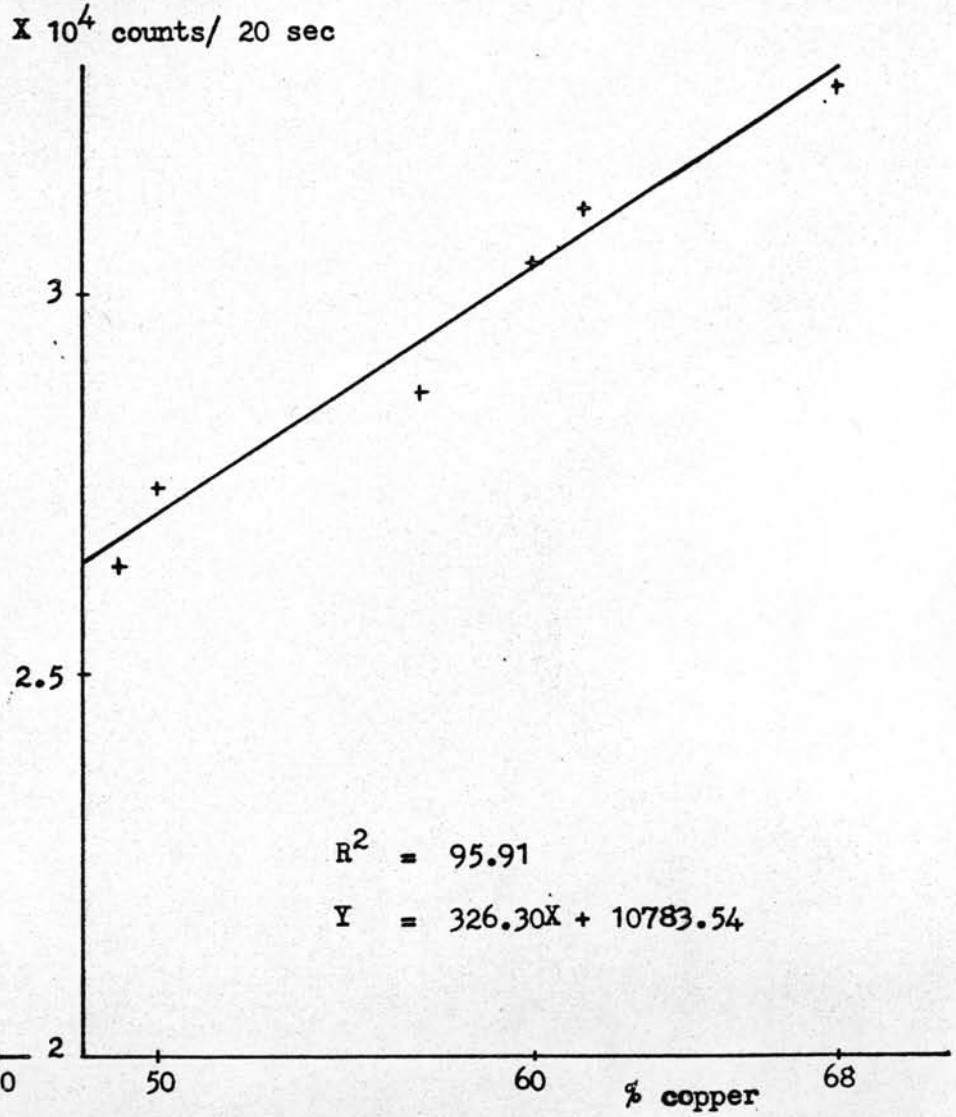

Fig. 18 Calibration curve shows relation between Peak area and % copper in Cast Copper Alloys.

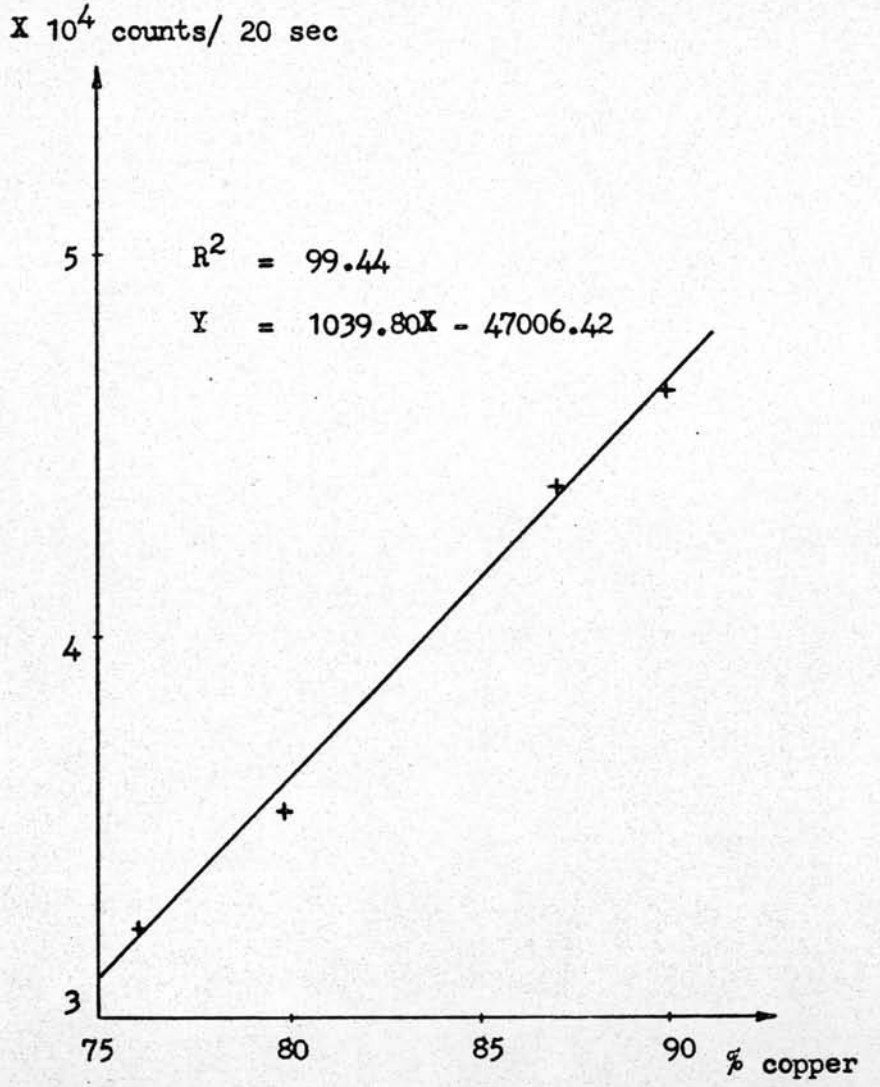

Fig. 19 Calibration curve shows relation between Peak area and % copper in Cast Aluminium Bronzes.

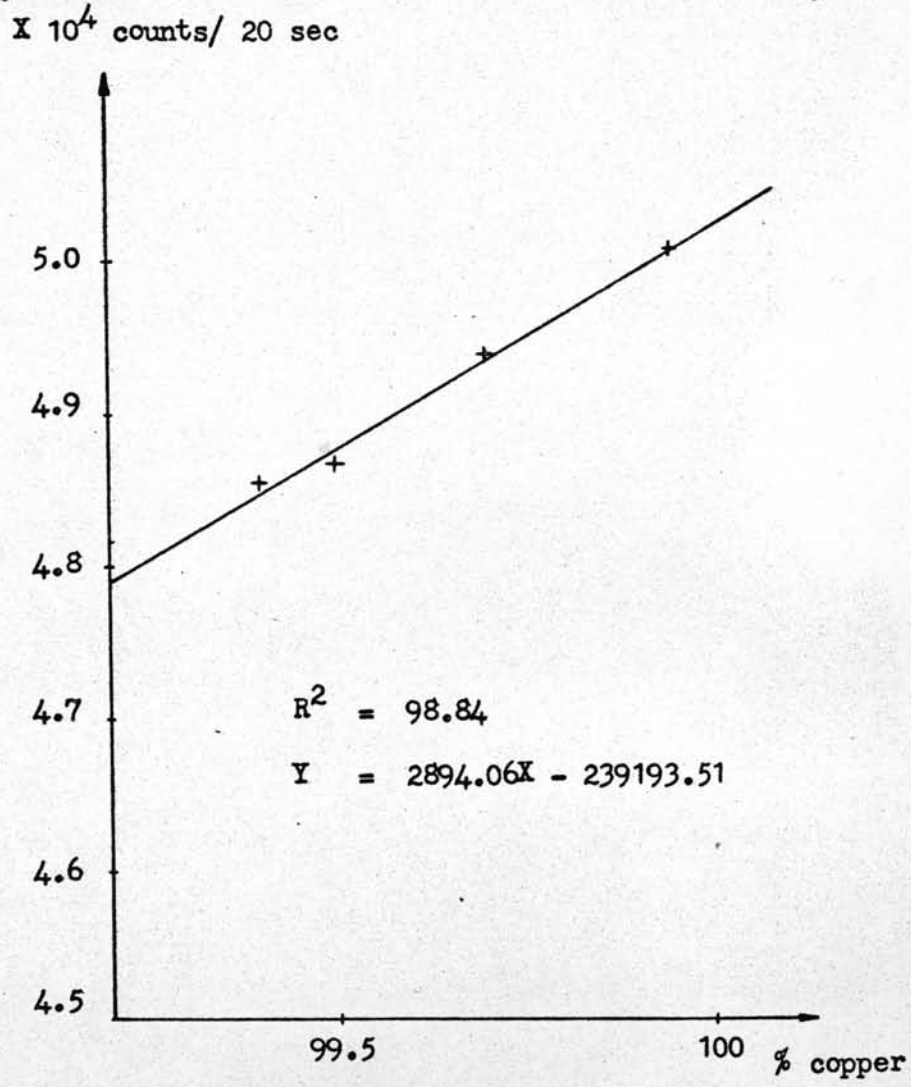

Fig. 20 Calibration curve shows relation between Peak area and % copper in nearly pure Copper.

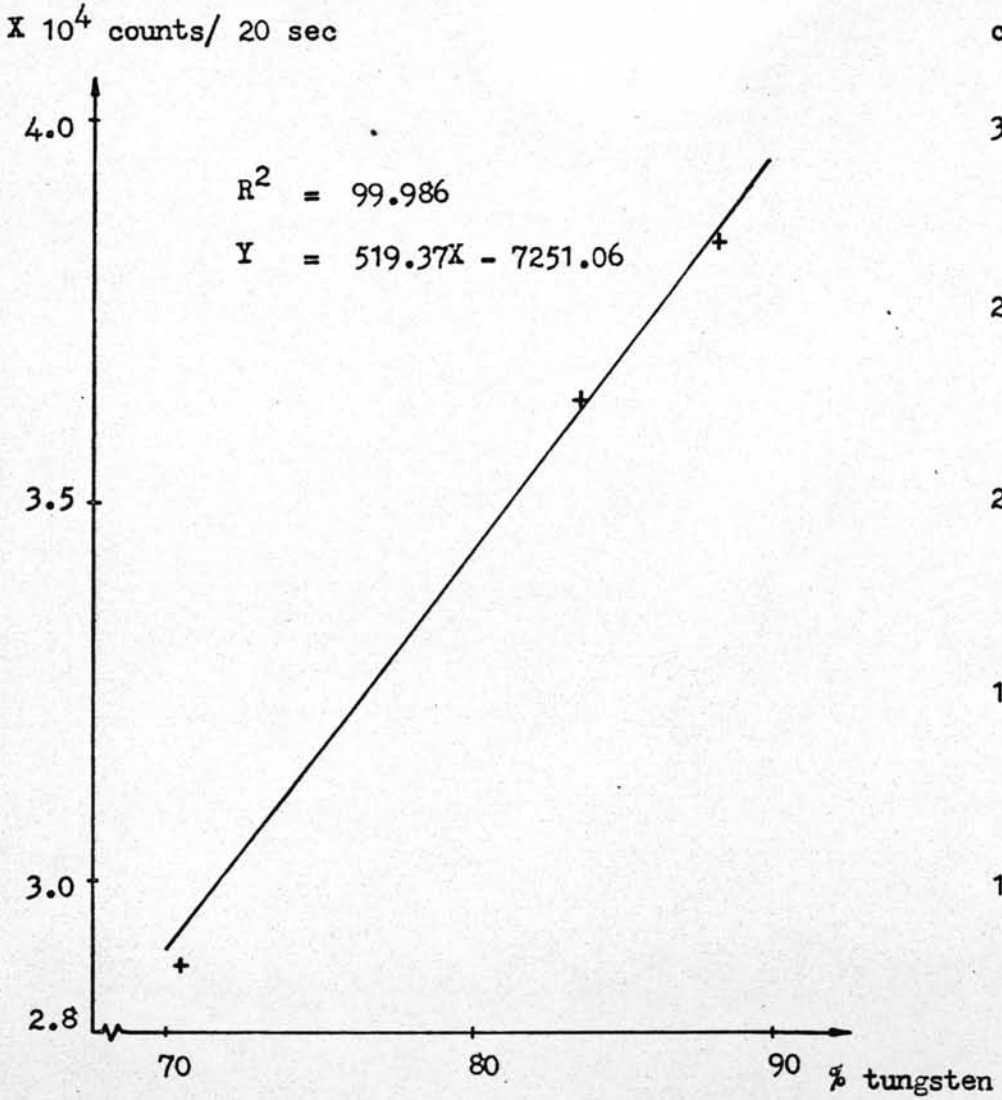

Fig. 21 Calibration curve shows relation between Peak area and % tungsten in Sintered Carbides.

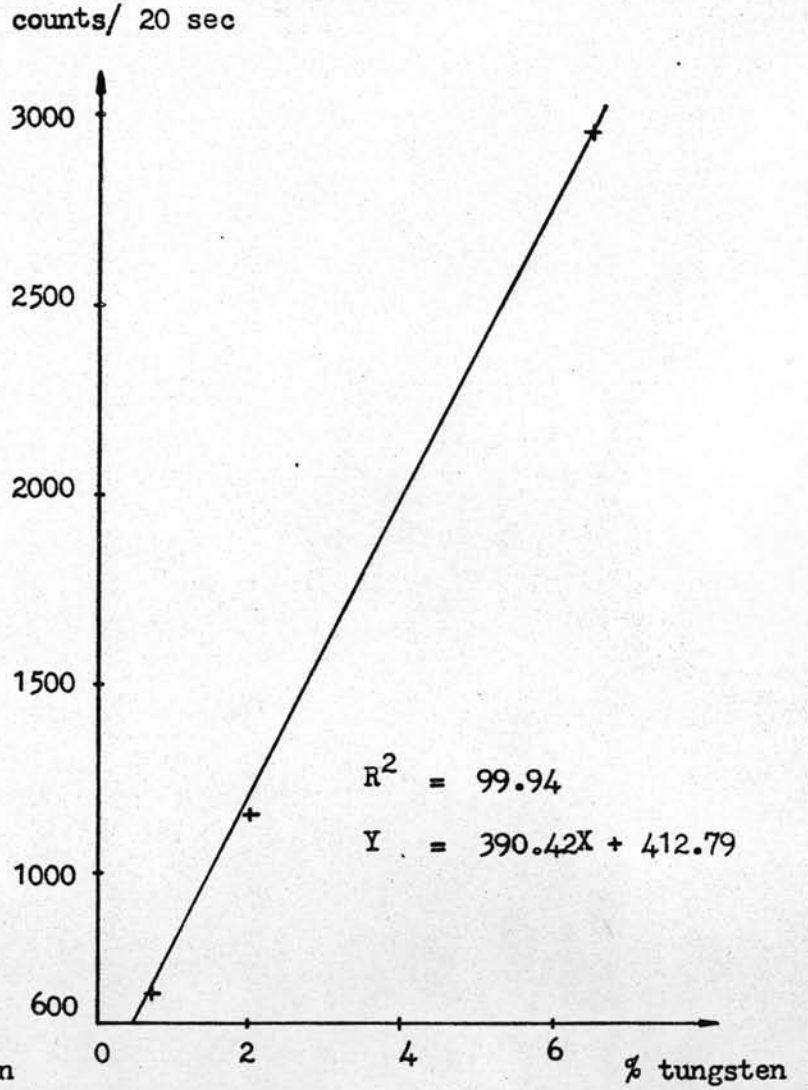

Fig. 22 Calibration curve shows relation between Peak area and % tungsten in Low Alloys Steels.